



**PANIC detector
characterization**

Doc.Ref: PANIC-DET-TR-01
Issue: 2.1
Date: 16.07.2015
Page 1 / 20



PANIC

PANIC Detector characterization

Prepared by	Bernhard Dörner Johana Panduro	Max-Planck-Institut für Astronomie
Checked by by		

Code: PANIC-DET-TR-01
Issue/Ver.: 2.1
Date: 16.07.2015
No. of pages: 20

	PANIC detector characterization	Doc.Ref: PANIC-DET-TR-01 Issue: 2.1 Date: 16.07.2015 Page 2 / 20
---	--	---

Document Change Log

Version	Date	Chapters affected	Comments
Issue 1.0	05.12.2012	All	First edition
Issue 2.0 draft0	13.02.2105	All	New layout, data from CAHA, still missing: persistence, crosstalk
Issue 2.0	26.03.2015	3, 9, 10	Added persistence and crosstalk
Issue 2.1	16.07.2015	3, 6.3, 7 11	Added noise+hot pixel data from 11 May 2015, removed evolution plots Added reference to bad pixel map comparison

List of acronyms and abbreviations

ADU	Analog-Digital Unit
FPA	Focal Plane Array
CDS	Correlated Double Sampling
PANIC	P Anoramic N ear Infrared camera for C alar A lto
ROE	Read-out Electronics
QE	Quantum Efficiency
CAHA	Centro Astronomico Hispano Aleman
SG	Science Grade

List of supporting documents

The following documents provide additional information about topics addressed in this document. They are referenced as RDx in the text:

RD Nr.	Identifier	Title	Issue	Date
RD 1	PANIC-DET-TN-02	PANIC detector non-linearity and correction data	1.0	19.02.2015
RD 2	PANIC-DET-TN-01	PANIC detector and readout features	1.0	20.02.2015
RD 3		PANIC Mosaic Characterization & Performance Report		05.12.2012



**PANIC detector
characterization**

Doc.Ref:
Issue:
Date:
Page 3 / 20

PANIC-DET-TR-01
2.1
16.07.2015

RD 4	doi: 10.1063/ 1.4733534	JWST near-infrared detector degradation— finding the problem, fixing the problem, and moving forward		
RD 5		H2RG SWIR SCA Test Report: PANIC-SG1 to 4		
RD 6	PANIC-OPT-TN-00	Signal to Noise cases	0.0	01.03.2007
RD 7	PANIC-OPT-SP-01	PANIC's Optical Final Design Report	0.1	10.09.2008
RD 8	PANIC-DET-TP-01	PANIC list of instrument test procedures	1.0	09.02.2015
RD 9	PANIC-DET-TR-05	PANIC detector pixel quality evolution	1.0	14.07.2015
RD 10	PANIC-DET-TR-06	PANIC comparison of bad pixel masks	1.0	16.07.2015



**PANIC detector
characterization**

Doc.Ref: PANIC-DET-TR-01
Issue: 2.1
Date: 16.07.2015
Page 4 / 20

Contents

1	Introduction and scope	5
1.1	General	5
1.2	Discussed items	5
2	Setup and data	5
2.1	Instrument setup	5
2.2	Detector setup	5
2.3	Data	6
3	Summary	6
4	Gain	7
5	Saturation	9
5.1	Full well	9
5.2	Usable range	9
6	Dark current and hot pixels	10
6.1	Dark current measurement	10
6.2	Dark current characteristics	12
6.3	Hot pixel numbers	12
7	Readnoise	14
8	Flatfield statistics	15
9	Persistence	16
10	Crosstalk	18
10.1	Interpixel crosstalk	18
10.2	Channel crosstalk	19
11	Bad pixel map	19



1 INTRODUCTION AND SCOPE

1.1 General

The PANIC Focal Plane Array (FPA) consists of four Teledyne HAWAII-2RG detectors assembled in a 2x2 mosaic. It covers the instrument field of view with a sampling of 4096x4096 pixels.

This document summarizes the detector characterization and performance data as measured during the cryogenic cycles in 2014 and 2015, including the last results from tests after the instrument repair in spring 2015.

1.2 Discussed items

The general characteristics discussed are gain, full well size, read noise, dark current, flatfield statistics, persistence, and crosstalk. The inherent non-linear behavior of the detectors is described separately in RD1 along with the recipe for correction. Aside from the described items, there are some features visible in the readout data, analyzed in RD 2.

2 SETUP AND DATA

2.1 Instrument setup

For most of the final characterization, PANIC was in operational configuration (all optical elements and detector integrated). For the crosstalk and persistence, the differences were:

- The filter wheels were not populated with the science filters, instead the damaged Ks and the O2K H with diffusor were installed in wheel 1
- The focal plane mask was mounted at the mirror structure entrance instead of the field stop

To illuminate the detector, a desk lamp was placed on top of the telescope adaptor. To create different intensities, it could be furnished with bulbs of different power, and the input voltage could be set with a stabilized power supply.

2.2 Detector setup

The voltages of the detector setup are listed in Table 1. They are the same as used for the data in RD 3, where the numbers given there for Vreset and Dsub are incorrect. The GEIRS and pattern version of the exposures is also in Table 1 (unless noted otherwise).

Table 1: Detector voltages and bit settings (pattern r73M, r77M, r78(M))

Parameter	SG1	SG2	SG3	SG4
Vext / V (bit)	2.6855 (2750)	2.6855 (2750)	2.6855 (2750)	2.6855 (2750)
Dsub / V (bit)	1.7441 (3800)	1.7441 (3800)	1.7441 (3800)	1.7441 (3800)
Vreset / V (bit)	1.1934 (2600)	1.1934 (2600)	1.1934 (2600)	1.1934 (2600)
Vbias gate / V (bit)	2.1997 (3604)	2.1997 (3604)	2.1997 (3604)	2.1997 (3604)
GEIRS	rjm_r726M-r-s64 (Oct 30 2014, 17:24:44), Panic_r78 (unless noted)			



PANIC detector characterization

Doc.Ref: PANIC-DET-TR-01
Issue: 2.1
Date: 16.07.2015
Page 6 / 20

The pixel clock was set to 100kHz. The minimum integration times with this patterns are

- lir: 2.739931s
- rrr-mpia: 1.370302s

2.3 Data

The characterization has been performed with various datasets. In every cold cycle, aside from special test and calibration data, a basic set has been recorded consisting of

- Dark images with shortest integration time
- Series of dark images with increasing integration time or up-the-ramp cubes
- Series of flatfield images with increasing integration time or up-the-ramp cubes

The individual procedures are listed in RD 8. The ones analyzed in detail are mentioned later on in the specific parts. The spreadsheets with the individual exposures are stored in the PANIC Power folder in Lab-Data/Detectors/Exposures/Procedures, or on the PANIC computers in /data1/ARCHIVE/PANIC/Procedures.

The data is stored in the directories listed in RD 8, and accessible on the PANIC computers at /data1/ARCHIVE/PANIC. In general, multiple exposures have been taken for each setting, and averaged with median and sigma clipping to increase the SNR per pixel, unless noted otherwise.

3 SUMMARY

The main results are summarized in Table 2. Since lir mode is preferred for operations, only results of this readmode are listed.

Table 2: Summary of characterization results for lir mode

Quantity for lir	SG1	SG2	SG3	SG4
Gain / e-/ADU	4.84	4.99	5.02	5.45
Full well / e-	266,000	264,000	260,000	251,000
Usable range / ADU	52,239	50,753	50,932	43,419
Usable range / e-	253,000	253,000	255,000	237,000
Linearity error <5%	<20,000 ADU	<20,000 ADU	<20,000 ADU	<20,000 ADU
Linearity error after correction (full range)	<1%	<1%	<1%	<1%
Readnoise / e-	16.7 ± 3.7	16.1 ± 3.4	17.7 ± 4.2	17.9 ± 3.9
Dark current mode / e-/s	0.164	0.234	0.269	1.330
Super-hot active pixels (>25,000 e-/s)	0.07%	0.38%	1.70%	9.93%
Hot active pixels (>5,000 e-/s)	0.15%	1.05%	3.78%	20.56%
Low QE active pixels	0.02%	0.29%	0.17%	0.14%

	PANIC detector characterization	Doc.Ref: PANIC-DET-TR-01 Issue: 2.1 Date: 16.07.2015 Page 7 / 20
---	--	---

Persistence ¹ (5min after saturation)	0.012%	0.059%	0.002%	N/A
Pixel crosstalk ¹ (left+right)	1.92%	1.47%	1.49%	3.95%
Channel crosstalk ¹ (saturated spot, bright ghost)	0.06%	0.09%	0.17%	N/A

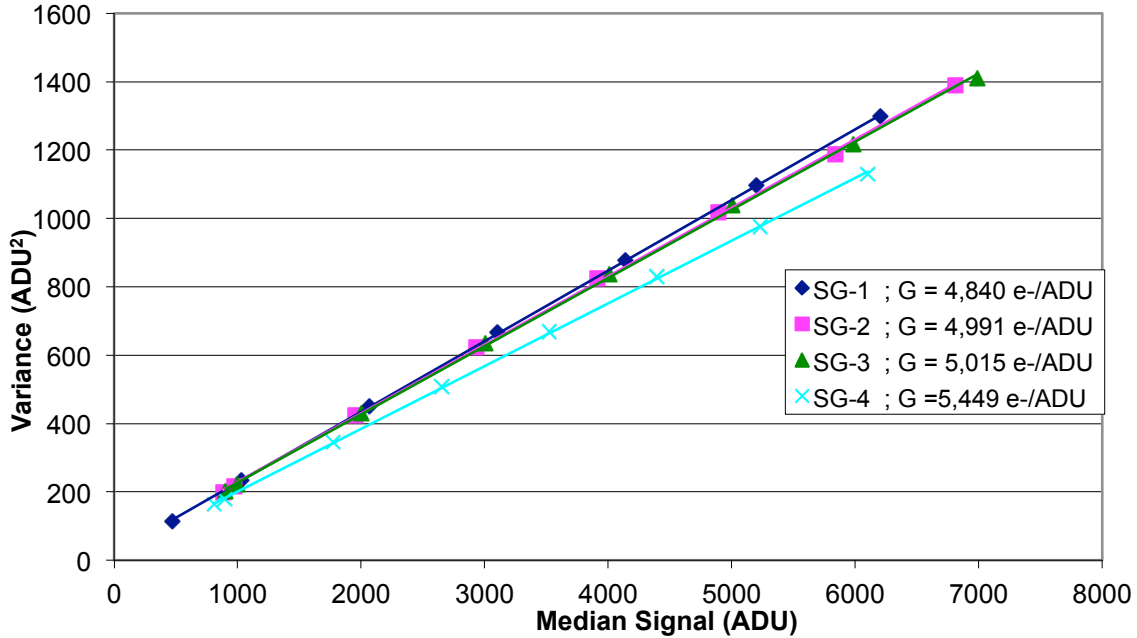
4 GAIN

The gain was measured from the data of DET_FLAT_3_3_asrun20141101 within the 1000x1000 px center area of each detector. Bad pixels determined from the linearity analysis (RD 1) were ignored.

With the photon transfer method, the gain results from the slope when plotting the noise vs the measured signal, as shown in Figure 1 for lir and rrr-mpia readmodes. The numbers are listed in Table 3.

¹ Measured with GEIRS rjm_r720M-r-s64 (Jul 2 2014, 10:12:28), Panic_r77M

**PANIC Mosaic: Gain (1000x1000 pix region pro Detector)
Comparison all detectors (lir) - 05.12.2014**



**PANIC Mosaic: Gain (1000x1000 pix region pro Detector)
Comparison all detectors (rrr-mpia) - 05.12.2014**

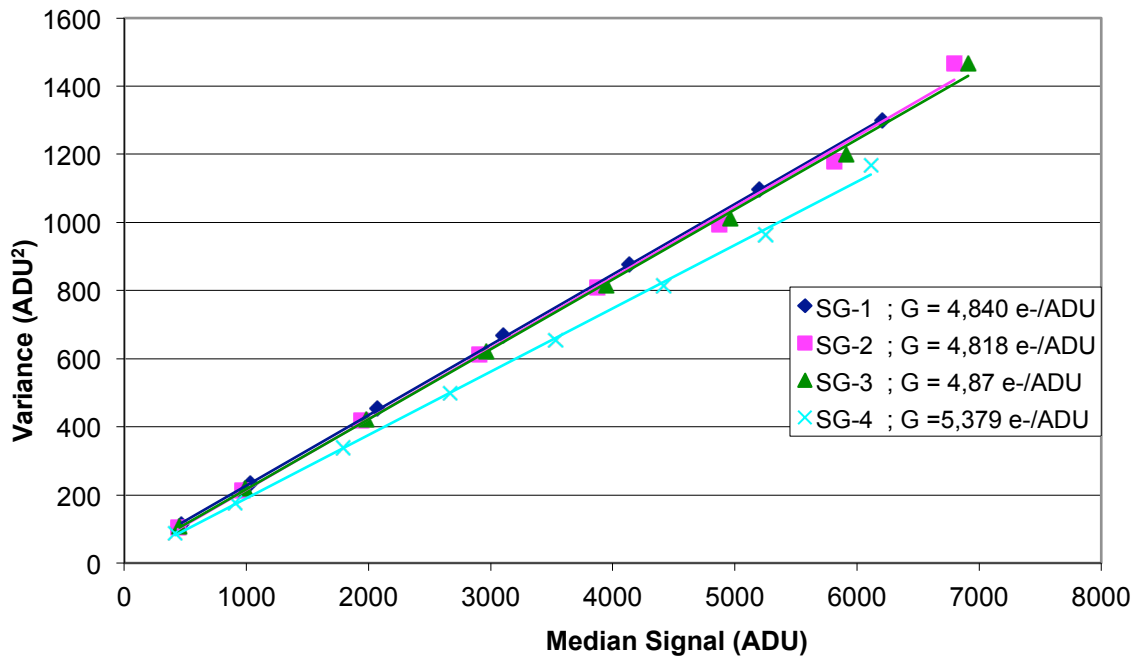


Figure 1: Photon transfer curve for gain measurement in modes lir (top) and rrr-mpia (bottom).

Table 3: Measured gain values

Gain / e-/ADU	SG1	SG2	SG3	SG4
lir	4.840	4.991	5.015	5.449
rrr-mpia	4.840	4.818	4.870	5.379

The values are similar for both modes, but more reliable for lir due to the better linear fit.

5 SATURATION

5.1 Full well

The pixel full well has been determined from data of the procedure DET_FLAT 3.3 in cycle 7 on 02/11/2014. For each exposure time, the median value of each detector has been calculated. The data levels out towards the long integration times (example in Figure 2). The numbers of the longest images for lir and rrr-mpia readout are listed in Table 4.

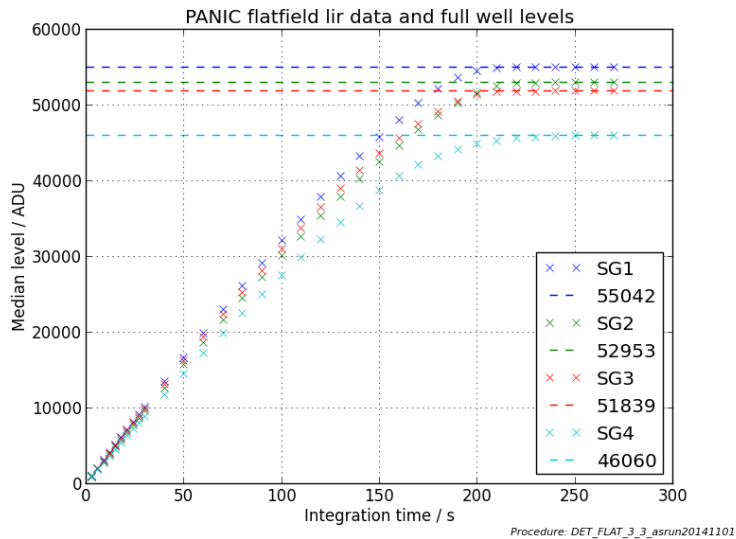


Figure 2: Median flatfield data for increasing integration times in lir mode. The full well is reached at the longest time.

Table 4: Median CDS full well capacity of each detector in readmodes lir and rrr-mpia.

Full well		SG1	SG2	SG3	SG4
lir median	ADU	55,042	52,953	51,839	46,060
	e ⁻	266,403	264,288	259,973	250,981
rrr-mpia median	ADU	50,179	49,269	46,873	42,339
	e ⁻	242,866	237,378	228,272	227,741

The full well is reached at about 250–266 ke⁻ for lir, and 228–243 ke⁻ for rrr-mpia. The values in ADU vary stronger due to the different gains. The larger well in lir mode is caused by the more pronounced reset drift for bright pixels (RD 2).

5.2 Usable range

Contrary to the full well limit, the usable range of the detectors is limited by the validity of the linearity correction. For the calibration of this effect, the maximum allowed signal was set to be at most 96% of the saturation. Depending on the quality of the ramp fits, it may even be lower. Figure 3 shows the histogram of the limits per detector in lir mode.

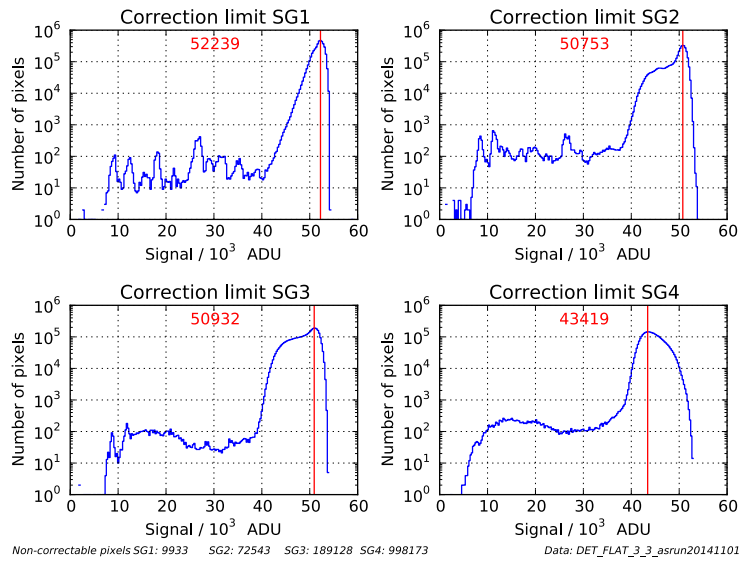


Figure 3: Maximum usable range for linearity correction in lir mode

The modes of the distribution are very close to 96% of the full well, indicating that the linearity calibration does not decrease the usable range more than intended.

Table 5 lists the correction limits for the two readmodes, as measured in CDS and linearized. Again, lir has a about 10% larger saturation limit.

The deviation from a linear signal is up to 5% in the range <20,000 ADU. After correction, it is typically <1% for the full usable range. Further details can be found in RD 1.

Table 5: Usable range for linearity correction: CDS measured counts, and linearized counts

Usable range			SG1	SG2	SG3	SG4
lir	Mode	ADU	52,239	50,753	50,932	43,419
		e ⁻	252,837	253,308	255,424	236,590
	Mode	ADU	61,952	62,736	62,825	53,080
	linearized	e ⁻	299,848	313,115	315,067	289,233
rrr-mpia	Mode	ADU	48,130	47,186	45,790	40,103
		e ⁻	232,949	227,342	222,997	215,703
	Mode	ADU	54,432	55,620	54,670	48,959
	linearized	e ⁻	263,450	267,977	266.243	263,350

6 DARK CURRENT AND HOT PIXELS

6.1 Dark current measurement

The dark current is difficult to quantify. The arrays in the PANIC FPA suffer from degradation known for this family of HAWAII-2RGs (RD 4). The effect manifests itself in a strongly elevated dark current, also leading to an increase of the hot pixel population. However, the dark signal has a very non-linear behavior, similar to discharging a capacitor. Therefore the dark count rates are different when measured with different exposure times.



PANIC detector characterization

Doc.Ref: PANIC-DET-TR-01
 Issue: 2.1
 Date: 16.07.2015
 Page 11 / 20

In detail this can be seen in up-the-ramp data dark cubes taken with DET_DARK_SHORT 1.1 in cycle 7 on 01/11/2014. The srr-cubes (for rrr-mpia) are composed of 61 frames with 2.5 s intervals, giving 150 s total exposure time. The lisrr-cubes (for lir) are composed of 112 frames during the shortest integration time of 153.473 s.

The reset frame was subtracted from all frames. Data above the saturation limit (96% full well from section 5.1) was rejected, and a straight line was fitted to the ramp of each pixel.

The pixels were grouped in a histogram after their dark rate, which are shown in Figure 4. The values of the median and the mode (histogram peak) are listed in Table 6.

Table 6: Linear dark current values from up-the-ramp cubes. The large population of degraded pixels distorts the distribution of SG3 and SG4, leading to a median very different from the mode.

Dark current		SG1	SG2	SG3	SG4
lir	mode / e-/s	0.164	0.234	0.269	1.330
	median / e-/s	0.174	0.314	0.714	17.588
rrr-mpia	mode / e-/s	0.041	0.094	0.129	1.090
	median / e-/s	0.044	0.167	0.567	17.293

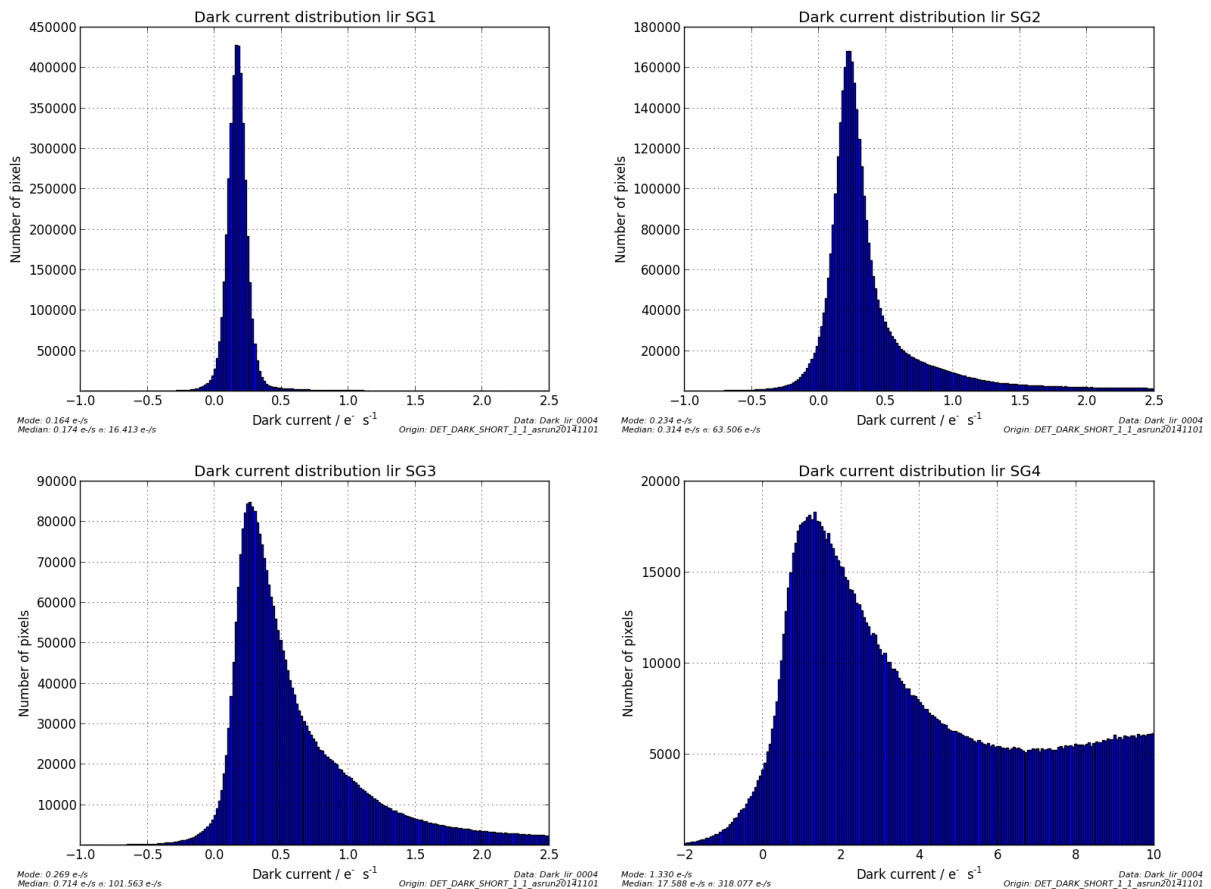


Figure 4: Dark rate histograms lir mode from lisrr-cube. Note the different x-range for SG4.

In each mode, the numbers match only for SG1 and SG2. In SG3, and even more SG4, the large population of degraded pixels with high dark current values distorts the distribution and therefore the median.

The values of the two modes are different, but on low levels. Although the numbers for SG1 and SG2 appear small, they are still significantly larger than the original specification of 0.01 e-/s (RD 5).

6.2 Dark current characteristics

The measurement of the dark current for levels >1 e-/s is further complicated by the nonlinear behavior of degraded pixels. Taking all pixels in SG1 in the lisrr-histogram bin around 5 e-/s, and plotting their mean and standard deviation in Figure 5, it is obvious that already small levels have a steeper rise at the beginning, and approach a constant rate later on. Also, the large standard deviation suggests that there can be pixels with a much higher initial increase.

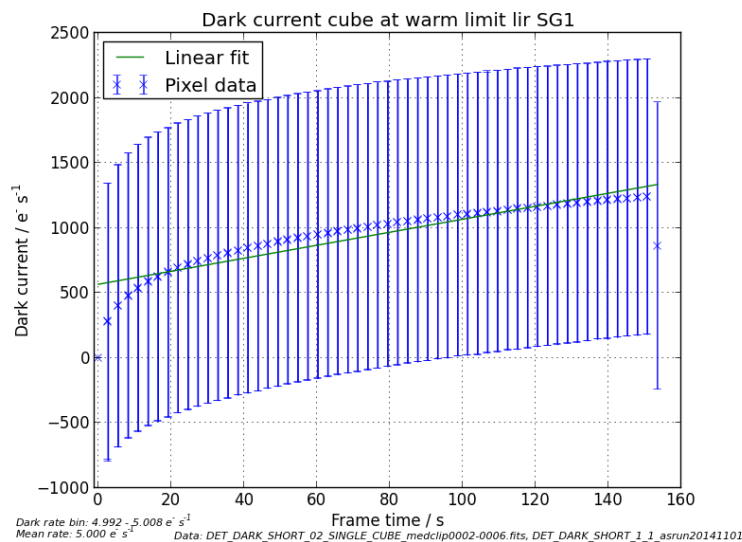


Figure 5: Dark current in SG1 around 5 e-/s: Mean pixel level and mean linear fit. The fit line does not represent the initial rise and later leveling. The drop in the last point is possibly due to a readout effect.

If the dark is now only fitted with a straight line, the values are wrong. Also if only one exposure time is used for the linear fit, it will produce wrong values for all other times. Therefore, it is recommended to take dark exposures with the same integration time as the science exposures from which they are subtracted.

6.3 Hot pixel numbers

The limits for hot pixels can be derived by setting a limit on the noise contribution. Taking the sky brightnesses in J/H/Ks reported in RD 6, the telescope collecting area from the CAHA website, a telescope and instrument throughput of 0.9 and 0.55 (RD 7), the nominal pixel scales (RD 7), and detector QE of 0.75 (RD 5), the following sky background electron rates are expected for the two CAHA telescopes:

Table 7: Expected sky signal per pixel for the 2.2m and 3.5m telescopes in the infrared bands

Band	T2.2 sky count rate / e-/s/pixel	T3.5 sky count rate / e-/s/pixel
J	3589	2298

	PANIC detector characterization	Doc.Ref: PANIC-DET-TR-01 Issue: 2.1 Date: 16.07.2015 Page 13 / 20
---	--	--

H	13879	8887
Ks	30151	19307

Once the dark electron rate becomes comparable to the sky background, the dark shot noise becomes significant and reduces the SNR. Therefore, the following limits are set to characterize the pixels:

- Super-hot pixels: >25,000 e⁻/s, saturating 250 ke⁻ in 10s
- Hot pixels: >2,500 e⁻/s, saturating 250 ke⁻ in 100s
- Warm pixels: >5 e⁻/s, saturating 250 ke⁻ in 50,000s

Judging only from the count rates, hot pixels are critical for the bands J and shorter, while some of them may be acceptable for H and Ks.

Unfortunately, the nonlinear dark behavior makes it impossible to properly quantify the pixels this way. As a workaround, these limits are evaluated with data taken with the minimum integration time (lir: 2.74s, rrr-mpia: 1.37s). Such data is also available from past detector tests and allows tracking the evolution of the arrays (see RD 9). The latest population fractions in the active pixels from the measurement with DET_NOISE 1.2 in cycle 9 on 11/05/2015 (after the instrument repair) are as shown in Table 8.

Table 8: Active hot pixel fractions in lir mode from 11/05/2015

Pixel type	SG1 fraction / %	SG2 fraction / %	SG3 fraction / %	SG4 fraction / %
Super-hot	0.07	0.38	1.70	9.93
Hot	0.15	1.05	3.78	20.56
Warm	2.42	22.77	73.15	87.27

The fraction of hot pixels is low in SG1, a little higher in SG2, elevated in SG3, and has passed critical levels in SG4, making this array largely unusable. The number of warm pixels seems very high for all detectors. Apparently, the low rate is exceeded during the 2.74s integration for many pixels. The dark current rate reduces with increasing exposure time (as apparent in Figure 5), otherwise the dark rate mode would not be below the 5 e⁻/s. Estimating the warm pixel fraction from the short exposure data is not very meaningful. The super-hot and hot values for the rrr-mpia mode are very similar, differences are <1%. The fractions of warm pixels are different, but also not reliable from the short integrations.

To observe the detector degradation over time, the hot and super-hot populations have been measured in older detector characterization data with short lir exposures. Details can be found in RD 9. Thanks to the almost continuously cold storage since the arrival at CAHA, the degradation effect has slowed down significantly. Also the fast warmup during the accident and the following short warm phase has not affected the status.

To conserve the detector health the best way, the arrays must be stored at cold conditions as long as possible. The degradation effect has to be continuously monitored, and characterization data has to be taken at the end and start of each instrument operation cycle, and regularly when at the telescope (in intervals of about 6 months).

7 READNOISE

The CDS read noise has been measured with the data from second run of DET_NOISE 1.2 in cycle 7 on 31/10/2014. For this, exposures 2–30 with shortest integration time have been stacked, and the standard deviation for each pixel was calculated.

The measurement is distorted in particular in SG4 due to the high dark current, and the values represent the shot noise of the dark signal instead. To obtain meaningful numbers, a read noise histogram was created for each detector in the range 0–50 e⁻ using only pixels which are not marked as warm in the hot pixel analysis (rate ≤5e⁻/s). The distributions were fitted with a Gaussian curve. The individual plots for SG1–4 in lir mode are shown in Figure 6.

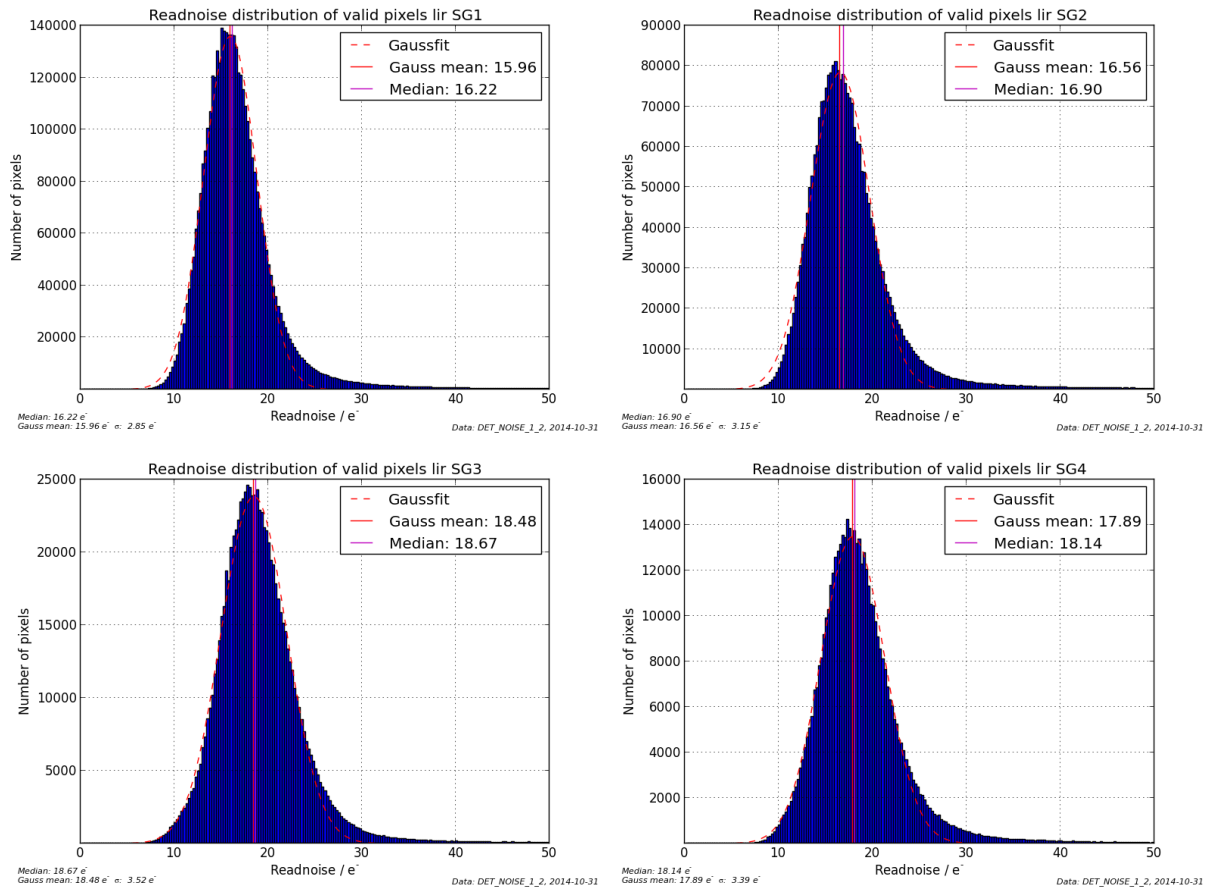


Figure 6: Read noise histograms SG1–4 lir mode and Gauss fits.

The distributions are slightly skewed towards larger values, but can be approximated with a Gaussian around the peak. The mean value and width of the fitted curves are given in Table 9.

Table 9: CDS read noise: Gaussian fit mean and width

Read noise / e ⁻	SG1	SG2	SG3	SG4
lir	16.7 ± 3.7	16.1 ± 3.4	17.7 ± 4.2	17.9 ± 3.9
rrr-mpia	16.5 ± 3.8	15.6 ± 3.3	17.9 ± 4.1	17.9 ± 3.9

The data of both modes match very well. The CDS readnoise is in the range expected for these detectors and similar to values from the Teledyne data sheets (RD 5).

To verify the instrument status, also the readnoise has been tracked over time. When only measuring healthy pixels, it is basically independent from the detector degradation seen in the dark current. Details can be found in RD 9.

8 FLATFIELD STATISTICS

From the data of the procedure DET_FLAT 3.3 in cycle 7 on 01/11/2014, the image with about 50% saturation was analyzed as a flatfield example. The histograms of the active pixels of each detector are plotted in Figure 7.

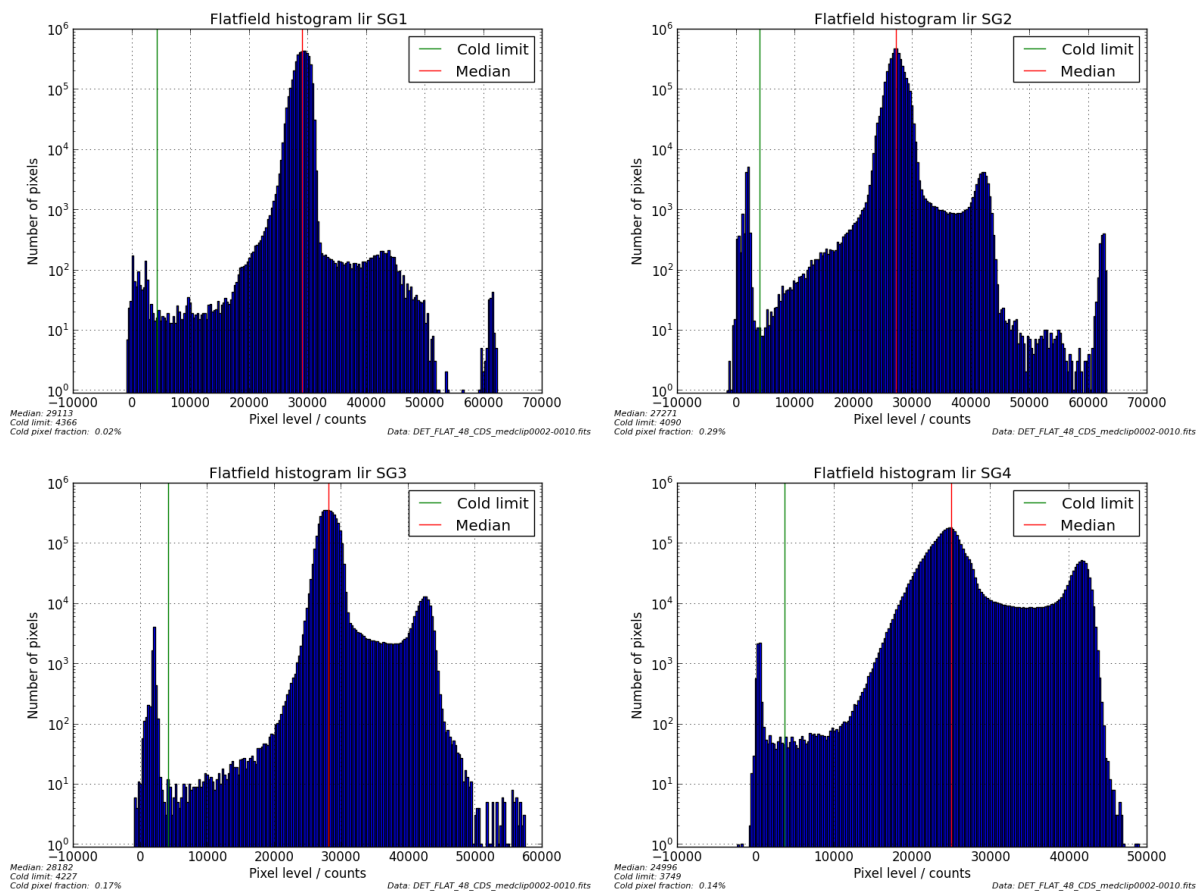


Figure 7: Histograms of lir flatfield image with about 50% saturation. The populations of low QE, normal, and hot pixels can be distinguished.

The median level is around 25–29,000 ADU for all detectors. The populations of hot pixels are visible on the high data end of the histogram. Another distinct group on the left side are pixels with low QE. Putting a limit of 15% of the median (green line), they can be selected in the histogram. The fractions are listed in Table 10, both readmodes lead to similar and very small values.

Table 10: Active pixel fractions with low QE (<15% median of flatfield)

Low QE pixels	SG1 fraction / %	SG2 fraction / %	SG3 fraction / %	SG4 fraction / %
---------------	------------------	------------------	------------------	------------------



PANIC detector characterization

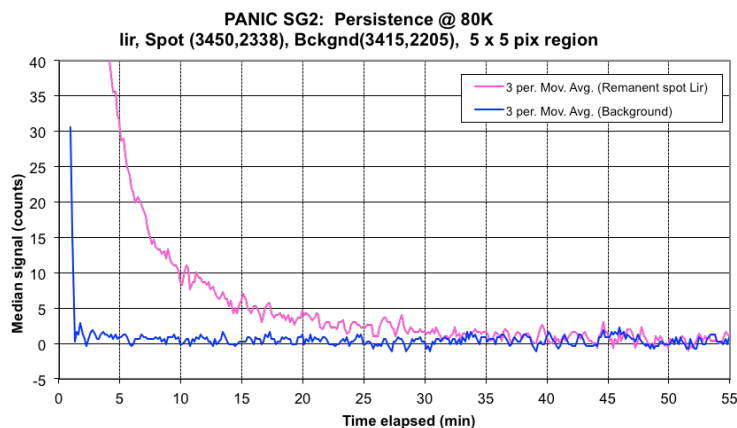
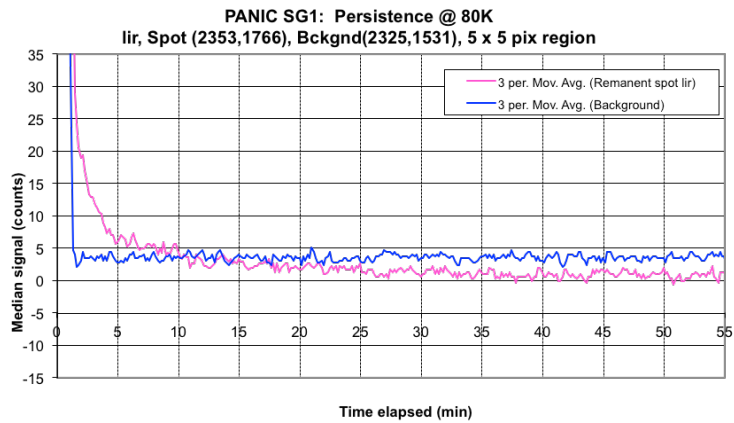
Doc.Ref: PANIC-DET-TR-01
Issue: 2.1
Date: 16.07.2015
Page 16 / 20

lir	0.02	0.29	0.17	0.14
rrr-mpia	0.02	0.28	0.17	0.14

9 PERSISTENCE

Persistence signals were measured with the data from DET_PERSISTENCE 2.0 on 10/07/2014 in cycle 4 with GEIRS rjm_r720M-r-s64 (Jul 2 2014, 10:12:28), Panic_r77M. Exposures were taken with the Ks filter and the focal mask at L1 installed. The pinhole images on each detector were analyzed, and compared to a non-illuminated background area. At first, 2 exposures were taken with 35 s to saturate the spots by about 10x. Then, with filters moved to BLANK, exposures of 10 s were taken for 55 min.

The median signals of the areas are plotted in Figure 8, normalized to the average signal at the end of the measurement. It was not possible to measure data in SG4 due to the large population of hot pixels.



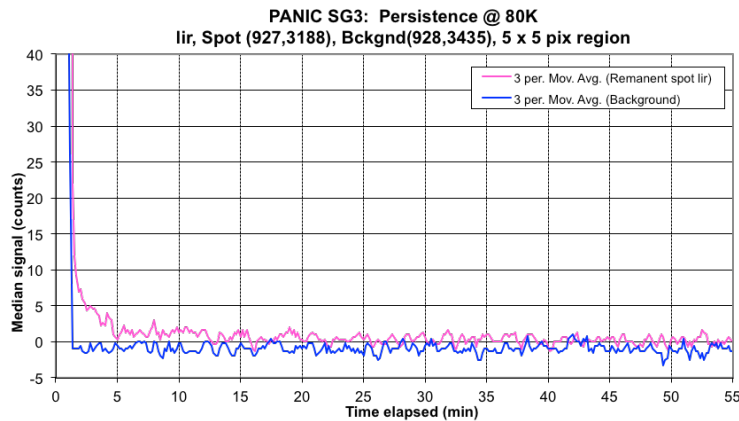


Figure 8: Persistence signal of 10x saturated spot in lir mode

The background signal has a constant offset with respect to the spot, and rather serves as estimation of the noise. This way it is possible to judge the time when the decay of the spots has ended. The signal fraction of the remnant spot for the two readmodes is listed in Table 11.

Table 11: Persistence measurement lir and rrr-mpia mode: intensity of remnant spot

Readmode	Elapsed time		Remnant spot / %		
	s	min	SG1	SG2	SG3
lir	60	1	0.16947	1.307264	0.07102
	120	2	0.03466	0.248191	0.01536
	300	5	0.01155	0.058732	0.00000
	420	7	0.00770	0.034103	0.00192
	540	9	0.00578	0.02463	0.00192
	600	10	0.00578	0.013262	0.00000
rrr-mpia	60	1	0.07474	0.33939	0.03765
	120	2	0.02828	0.08033	0.00837
	300	5	0.01212	0.02611	0.00418
	420	7	0.00606	0.01807	0.00209
	540	9	0.00404	0.01406	0.00209
	600	10	0.00606	0.01004	0.00000

The decay behavior is similar in both readmodes, if a little slower in lir. The counts in SG1 and 2 return to 0 within 15–20 min, SG2 has a longer decay time of about 40 min. Note that three points at 5 and 10 min are 0 since the measurement is 0, but the moving average in the plot yields a similar remnant amount as at 9 min.

10 CROSSTALK

10.1 Interpixel crosstalk

The pixel crosstalk was measured in data of cycle 7 DET_NOISE 1.2 recorded on the 31/10/2014, with GEIRS rjm_r726M-r-s64 (Oct 30 2014, 17:24:44), Panic_r78. In each detector, 10 hot pixels were selected, and the percentage in the direct neighbors calculated. One example image is shown in Figure 9.

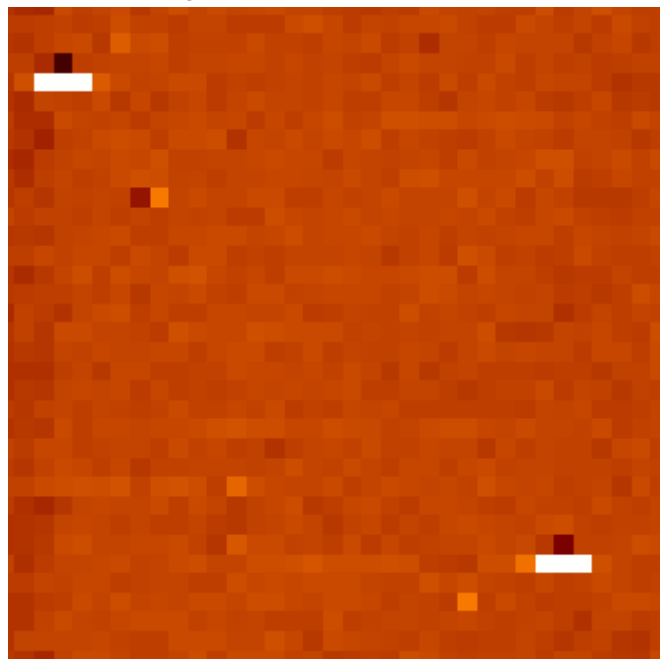


Figure 9: Example of pixel crosstalk around hot pixels in SG1, cuts: -72–110 ADU

The median values of the neighboring pixels are listed in Table 12. The overall values are comparable to the ones of the Teledyne test reports (1.6–2%). SG4 has slightly elevated numbers, resulting from the generally high fraction of hot pixels.

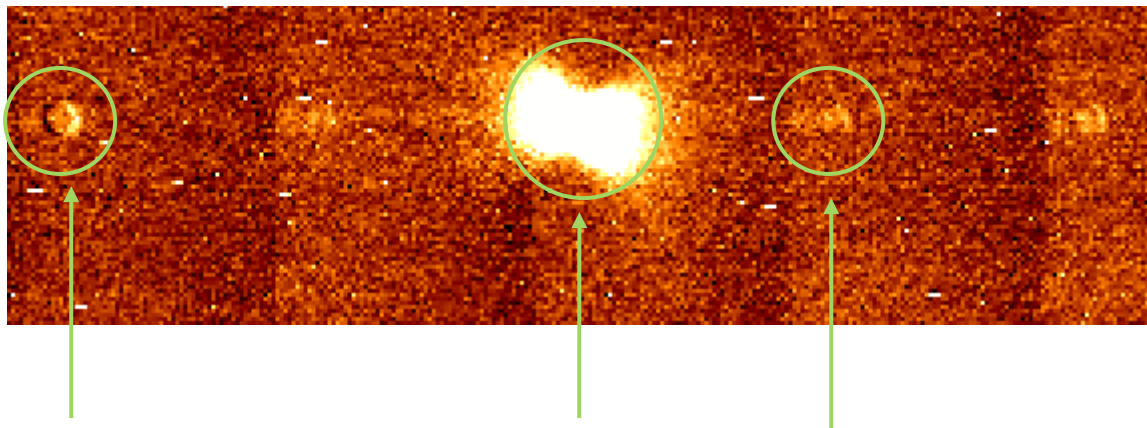
Table 12: Inter-pixel crosstalk

Readmode	Neighbor pixel	Median crosstalk / %			
		SG1	SG2	SG3	SG4
lir	Left	2.36	1.49	1.53	4.36
	Right	1.48	1.45	2.05	3.53
	Upper	-0.12	0.00	0.03	0.39
	Lower	-0.01	-0.15	-0.13	-0.13
rrr-mpia	Left	2.32	1.49	1.51	3.62
	Right	1.39	1.41	1.94	2.45
	Upper	1.18	-0.02	-0.00	1.78
	Lower	-0.11	0.84	1.33	-0.30

However, there is a clear difference between the upper+lower and left+right direction. This is also apparent in Figure 9, and most likely caused by the line reset used in PANIC. Note that the directions of SG2+3 in the image are inverted with respect to the directions of SG1+4 in the readout.

10.2 Channel crosstalk

The channel crosstalk was measured in data of cycle 4 DET_XTALK 1.0 recorded on the 10/07/2014, with GEIRS rjm_r720M-r-s64 (Jul 2 2014, 10:12:28), Panic_r77M. With the focal mask, spots in the image are taken at about saturation and with 10x saturation, and the intensities of ghosts appearing in the other channels are compared with the bright spot (Figure 10). SG4 could not be characterized due to the large amount of hot pixels. The results are listed in Table 13.



Major Ghost

Bright Spot

Faint Ghost

Figure 10: Image showing channel crosstalk: The saturated bright spot (center) appears at the conjugated positions in the other channels with different intensities (faint and major ghosts)

Table 13: Channel crosstalk for bright and faint electrical ghosts

Readmode	Ghost type	Fraction of bright spot / %					
		About saturation			10x saturation		
		SG1	SG2	SG3	SG1	SG2	SG3
lir	Major	0.06	0.09	0.17	0.18	0.19	0.27
	Faint	0.04	0.03	0.05	0.20	0.12	0.20
rrr-mpia	Major	0.12	0.08	0.15	0.24	0.16	0.25
	Faint	0.04	0.02	0.04	0.20	0.11	0.18

The readmodes show a very similar behavior. The ghosts are <0.2% for saturated points, and <0.3% for 10x saturated points.

11 BAD PIXEL MAP

The map of all bad pixels (hot, low QE) can be derived from the tests above. However, also the nonlinearity analysis provides a list of non-correctable pixels, which always will be considered invalid (RD 1). The selection criteria aim for the same pixel types, and the

fractions are close to the ones shown in this document. The populations are very similar as confirmed by a separate analysis in RD 10.

The image of the correction limit in lir mode is shown in Figure 11. The bad pixels are marked in red.

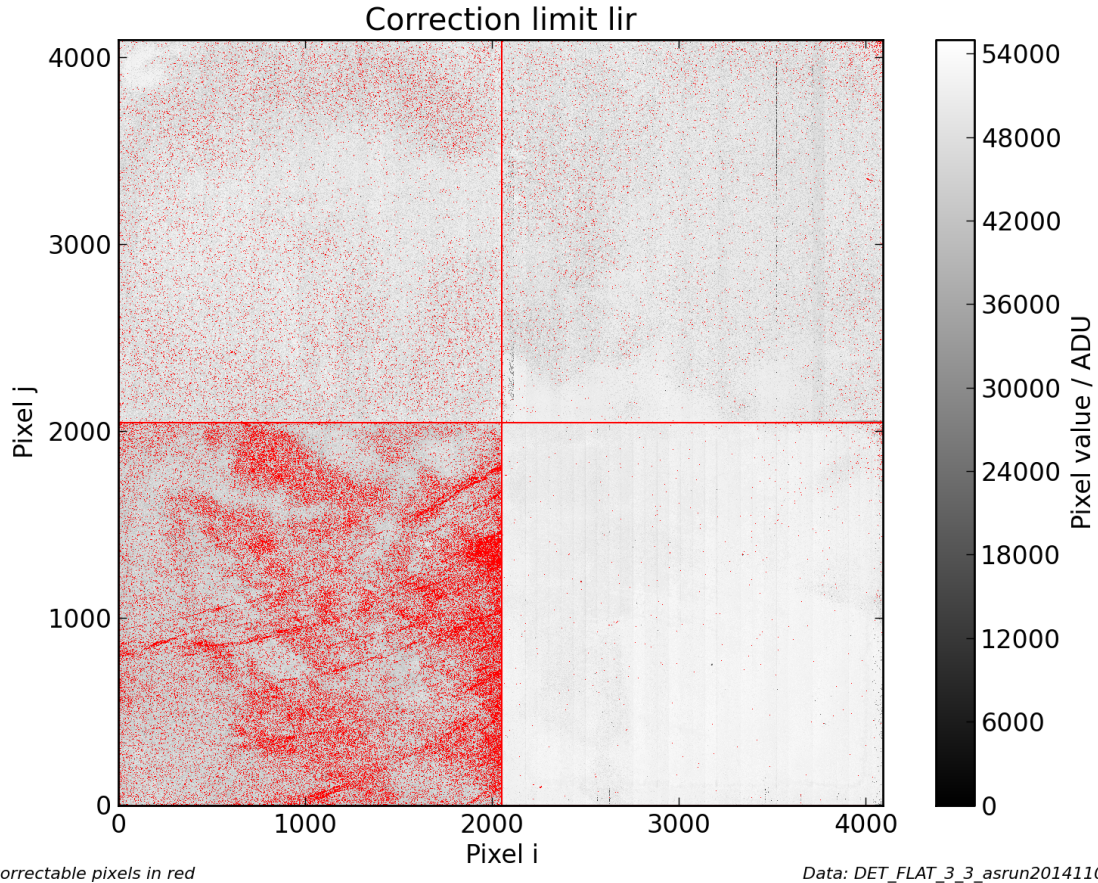


Figure 11: Map of lir mode linearity correction limit with bad pixels in red.

The clustering in SG4 is apparent, as well as the reference pixels around each detector. The information is stored in a FITS file, and also made available for GEIRS in a text file.